

# High efficiency THz generation in DSTMS, DAST and OH1 pumped by Cr:forsterite laser

C. Vicario,<sup>1,\*</sup> M. Jazbinsek,<sup>2</sup> A. V. Ovchinnikov,<sup>3</sup> O. V. Chefonov,<sup>3</sup> S. I. Ashitkov,<sup>3</sup> M. B. Agranat,<sup>3</sup> and C. P. Hauri<sup>1,4</sup>

<sup>1</sup>Paul Scherrer Institute, SwissFEL, 5232 Villigen PSI, Switzerland

<sup>2</sup>Rainbow Photonics AG, 8048 Zurich, Switzerland

<sup>3</sup>Joint Institute for High Temperatures of RAS, Izhorskaya st. 13 Bd. 2, Moscow 125412, Russia

<sup>4</sup>Ecole Polytechnique Federale de Lausanne, 1015 Lausanne, Switzerland

\*carlo.vicario@psi.ch

**Abstract:** We investigated Terahertz generation in organic crystals DSTMS, DAST and OH1 directly pumped by a Cr:forsterite laser at central wavelength of 1.25  $\mu\text{m}$ . This pump laser technology provides a laser-to-THz energy conversion efficiency higher than 3 percent. Phase-matching is demonstrated over a broad 0.1-8 THz frequency range. In our simple setup we achieved hundred  $\mu\text{J}$  pulses in tight focus resulting in electric and magnetic field larger than 10 MV/cm and 3 Tesla.

©2015 Optical Society of America

**OCIS codes:** (140.3070) Infrared and far-infrared lasers; (190.4710) Optical nonlinearities in organic materials; (190.7110) Ultrafast nonlinear optics; (260.3090) Infrared, far; (300.6495) Spectroscopy, terahertz.

---

## References and links

1. C. Vicario, B. Monoszalai, and C. P. Hauri, "GV/m Single-Cycle Terahertz Fields from a Laser-Driven Large-Size Partitioned Organic Crystal," *Phys. Rev. Lett.* **112**, 213901 (2014).
2. C. Ruchert, C. Vicario, and C. P. Hauri, "Spatiotemporal focusing dynamics of intense supercontinuum THz pulses," *Phys. Rev. Lett.* **110**(12), 123902 (2013).
3. C. Ruchert, C. Vicario, and C. P. Hauri, "Scaling submillimeter single-cycle transients toward megavolts per centimeter field strength via optical rectification in the organic crystal OH1," *Opt. Lett.* **37**(5), 899–901 (2012).
4. C. P. Hauri, C. Ruchert, C. Vicario, and F. Ardana-Lamas, "Strong-field single-cycle THz pulses generated in an organic crystal," *Appl. Phys. Lett.* **99**(16), 161116 (2011).
5. B. Monoszalai, C. Vicario, M. Jazbinsek, and C. P. Hauri, "High-energy terahertz pulses from organic crystals: DAST and DSTMS pumped at Ti:sapphire wavelength," *Opt. Lett.* **38**(23), 5106–5109 (2013).
6. C. Vicario, C. Ruchert, F. Ardana-Lamas, P. M. Derlet, B. Tudu, J. Luning, and C. P. Hauri, "Off-resonant magnetization dynamics phase-locked to an intense phase-stable terahertz transient," *Nat. Photonics* **7**(9), 720–723 (2013).
7. T. Kampfrath, K. Tanaka, and K. A. Nelson, "Resonant and nonresonant control over matter and light by intense terahertz transients," *Nat. Photonics* **7**(9), 680–690 (2013).
8. H. Y. Hwang, S. Fleischer, N. C. Brandt, B. G. Perkins, Jr., M. Liu, K. Fan, A. Sternbach, X. Zhang, R. D. Averitt, and K. A. Nelson, "A review of non-linear terahertz spectroscopy with ultrashort tabletop-laser pulses," *J. Mod. Opt.* **0**, 1–33 (2014).
9. M. Clerici, M. Peccianti, B. E. Schmidt, L. Caspani, M. Shalaby, M. Giguère, A. Lotti, A. Couairon, F. Légaré, T. Ozaki, D. Faccio, and R. Morandotti, "Wavelength scaling of Terahertz generation by gas ionization," *Phys. Rev. Lett.* **110**(25), 253901 (2013).
10. J. A. Fülöp, L. Pálfalvi, S. Klingebiel, G. Almási, F. Krausz, S. Karsch, and J. Hebling, "Generation of sub-mJ terahertz pulses by optical rectification," *Opt. Lett.* **37**(4), 557–559 (2012).
11. C. Vicario, B. Monoszalai, C. Lombosi, A. Mareczko, A. Courjaud, J. A. Fülöp, and C. P. Hauri, "Pump pulse width and temperature effects in lithium niobate for efficient THz generation," *Opt. Lett.* **38**(24), 5373–5376 (2013).
12. M. B. Agranat, S. I. Ashitkov, A. A. Ivanov, A. V. Konyashchenko, A. V. Ovchinnikov, and F. E. Fortov, "Terawatt femtosecond Cr : forsterite laser system," *Quantum Electron.* **34**(6), 506–508 (2004).
13. G. Arisholm, R. Paschotta, and T. Südmeyer, "Limits to the power scalability of high-gain optical parametric amplifiers," *J. Opt. Soc. Am. B* **21**, 578 (2004).
14. R. Kaneko, S. Kawabe, I. Kawayama, H. Murakami, Y. Takahashi, T. Shibuya, M. Yoshimura, K. Suizu, K. Kawase, Y. Mori, and M. Tonouchi, "Evaluation of organic crystal DASC and DAST for THz difference frequency generation using a cr: Forsterite laser," *Infrared, Millimeter and Terahertz Waves (IRMMW-THz)*, 2011 36th International Conference 1, 1, 2 Oct. 2011.

15. C. Vicario, A. V. Ovchinnikov, S. I. Ashitkov, M. B. Agranat, V. E. Fortov, and C. P. Hauri, "Generation of 0.9-mJ THz pulses in DSTMS pumped by a Cr:Mg<sub>2</sub>SiO<sub>4</sub> laser," *Opt. Lett.* **39**(23), 6632–6635 (2014).
16. A. Schneider, M. Neis, M. Stillhart, B. Ruiz, R. U. A. Khan, and P. Günter, "Generation of terahertz pulses through optical rectification in organic DAST crystals: theory and experiment," *J. Opt. Soc. Am. B* **23**(9), 1822 (2006).
17. L. Mutter, F. D. Brunner, Z. Yang, M. Jazbinšek, and P. Günter, "Linear and nonlinear optical properties of the organic crystal DSTMS," *J. Opt. Soc. Am. B* **24**(9), 2556 (2007).
18. F. D. Brunner, O. P. Kwon, S. J. Kwon, M. Jazbinšek, A. Schneider, and P. Günter, "A hydrogen-bonded organic nonlinear optical crystal for high-efficiency terahertz generation and detection," *Opt. Express* **16**(21), 16496–16508 (2008).
19. Electric field  $\xi_p$  of a pulse with energy  $E$  and duration  $\Delta t$  focused in a waist with radius  $r$ , is calculated from the formula:  $\xi_p = \sqrt{\xi_0 \cdot E / (2\pi \cdot r^2 \cdot \Delta t)}$  where  $\xi_0$  is the impedance of the free space  $\xi_0 = 1/c \cdot \epsilon_0$ , being  $c$  the speed of light and  $\epsilon_0$  the vacuum permittivity.
20. M. Shalaby and C. P. Hauri, "Terahertz brightness at the extreme: demonstration of a 5 GV/m, 17 T low frequency  $\lambda^3$  terahertz bullet" arXiv 1407.1656 (2014).

## 1. Introduction

Terahertz generation by optical rectification (OR) in nonlinear organic crystals (NOCs) has recently attracted considerable attention as they allow the production of ultrabroadband THz spectra in the low-frequency THz range (1–20 THz) [1–5]. OR in NOCs is exceptionally efficient with pump-to-THz energy conversion as high as few percent and large THz energy density per emitting area ( $>150 \mu\text{J}/\text{cm}^2$ ). In NOCs the emitted THz waveform is a phase-stable single-cycle pulse with unprecedented fields values (several MV/cm and Tesla for the electric and magnetic field) whose peak field strength is limited primarily by the available crystal size and pump power. These are important attributes and disclose new opportunities for the emerging field of THz nonlinear photonics. As an example recent table-top source developments have enabled time resolved exploration at unprecedented strong field [6–8].

THz sources with complementary properties are realized by means of a variety of laser technologies and nonlinear processes. Plasma-based sources, for example, offer broadband emission (1–100 THz) but limited pulse energy ( $\approx 0.1$ – $1 \mu\text{J}$ ) [9]. Large pulse energies ( $\approx 100 \mu\text{J}$ ) are achieved by OR in lithium niobate using tilted pulse front scheme and cryogenically cooled crystals but the spectral emission is confined to 0.1–1 THz [10, 11]. Exploration of novel OR materials and pump laser schemes is justified by the request of the steady increasing THz peak power and spectral output.

In this article we explore the THz emission properties in NOCs DSTMS, DAST and OH1 using a pumping scheme based on optical rectification of a femtosecond Cr:Mg<sub>2</sub>SiO<sub>4</sub> (Cr:F) amplified laser [12]. The pumping approach deviates from the conventional methodology for exciting NOCs by a drive laser based on (A) a Ti:sapphire-pumped high-energy optical parametric amplifier (OPA) emitting at wavelength  $\lambda = 1.3$ – $1.6 \mu\text{m}$  and beam polarizations utilizing the  $\chi_{111}^{\text{OR}}$  nonlinear susceptibility coefficient [1–4] or (B) Ti:sapphire emitting at  $\lambda = 0.8 \mu\text{m}$  utilizing the  $\chi_{122}^{\text{OR}}$  coefficient [5]. Whereas the latter offers straightforward THz generation, the related nIR-to-THz energy conversion efficiency is rather low ( $10^{-4}$ – $10^{-5}$ ). In the past, the pump approach (A) has been the most preferred as it offers two orders of magnitude higher conversion efficiency leading to highest THz pulse energies and peak fields. Beside intrinsic high conversion losses [13], the white-light seeded OPA are unfavorable for THz generation as their beam profiles are often affected by hot spots and transverse irregularities, which limit the maximum usable fluence to pump the organic crystals. Moreover the shot-to-shot amplitude fluctuation in the OPA results in often-unstable THz emission. Differently to the above mentioned pump schemes, the approach presented here is based on direct pumping of NOCs with a high-energy chirped-pulse amplification Cr:F laser system. Cr:F driven OR in NOCs combines the high conversion efficiency and high field realized with the pump scheme (A) while, similar to the approach (B), no additional frequency conversion scheme with intrinsic additional losses are needed. In fact, the emission

for Cr:F is peaked at mid-infrared wavelengths (1250 nm), which provide optimal velocity matching with the emitted THz beam in NOCs. As the Cr:F lases directly at near optimum pump wavelength for NOCs, it does not need multi-staged non-linear amplification processes in high-energy OPAs and offers furthermore a beam profile superior to (B). Experimentally this turns into higher conversion efficiency. The energy per pulse in Cr:F amplifier is one order of magnitude larger than the typical output from commercially available OPA. This pump technology has therefore the potential to generate mJ level THz energies by large-size NOCs.

In the past a Cr:F laser was used for difference-frequency generation in NOCs resulting in narrowband THz waves [14]. Here we demonstrate high-field and broadband THz emission by optical rectification in DSTMS, DAST and OH1. The crystals are directly pumped by a high-energy Cr:F laser, which delivers to the organic crystal up to 30 mJ, 100 fs pulses. In the following we present measurements on spectral content, conversion efficiency, field strength, focusing properties and discuss phase-matching conditions of OR at Cr:F wavelength. This work extends our previous study on the generation of THz pulse with energy as high as 900  $\mu$ J in large size mosaic patterned DSTMS pumped by Cr:forsterite used for high-field applications [15].

## 2. Coherence length at different pump wavelength in organic crystals

One of the recognized concepts for high-field Terahertz generation is based on efficient optical rectification in DAST, DSTMS and OH1 of femtosecond laser pulses at a wavelength between 1.35 and 1.5  $\mu$ m [1–4]. While this THz conversion scheme easily provides THz pulses of MV/cm field strength, it requires a sophisticated white-light seeded multi-stage OPA, which is pumped by a high-energy Ti:sapphire laser. Here we show a viable alternative for efficient THz generation by direct pumping the organic crystals with a Cr:F system at 1250 nm. At this wavelength the coherence length for THz-wave generation via optical rectification is sufficiently large over a large spectral bandwidth for high-efficiency conversion.

The high optical damage threshold and the feasibility to grow the organic crystals at relatively large size ( $\approx$ cm<sup>2</sup>) make them attractive for high field applications. They show broadband velocity matching between THz and a mid-infrared pump, a large non-resonant second-order nonlinear optical susceptibility and a high THz transmission when operated in simple, collinear pump geometry.

The ionic organic crystal 4-N-methylstilbazolium tosylate (DAST) has been developed in the 90s and extensively used for optical rectification because of its large second order nonlinearity [16]. The DSTMS is derived from the DAST by minor changes of the substituents of the counter-anion [17]. These modifications are shown to influence considerably the low frequency phonon absorption (1.1 THz) while keeping the high optical susceptibility. The DSTMS could partially overcome the discontinuity of the phonon frequency of DAST enabling broadband emission between 1 and 5 THz. Both crystals present best velocity matching in OR for pump wavelength at 1500 nm. The non-ionic organic crystal 2-[3-(4-hydroxystyryl)-5.5-dimethylcyclohex-2-enylidene] malononitrile OH1 [18], on the other hand, has been also identified as potential candidate for high energy THz source since its high nonlinear susceptibility. Furthermore OH1 presents low THz absorption from 0.3 to 3 THz and offers excellent velocity matching between THz and pump wavelengths at around 1.35  $\mu$ m. In the following we present a comparison of THz generation in these NOCs for the Cr:F pump and at other mid-infrared wavelengths. As figure of merit we calculate the coherence length  $l_c$  for optical rectification defined as:

$$l_c(v_{THz}, \lambda_p) = \frac{c}{2v_{THz} \cdot [n(v_{THz}) - n_g(\lambda_p)]} \quad (1)$$

where  $n(\nu_{\text{THz}})$  is the refractive index at the THz frequency  $\nu_{\text{THz}}$ , and  $n_g(\lambda_p)$  is the group index for the pump at the optical wavelength  $\lambda_p$ . We can determine the coherence length for the different organic crystals using the measured refractive and group indices. The two-dimensional representations of  $l_c$  at different  $\nu_{\text{THz}}$  as function of the pump wavelength in DAST, DSTMS and OH1 are displayed in Fig. 1. A better velocity matching and larger coherence length over the bandwidth supported by the pump pulse duration results in more efficient THz generation.

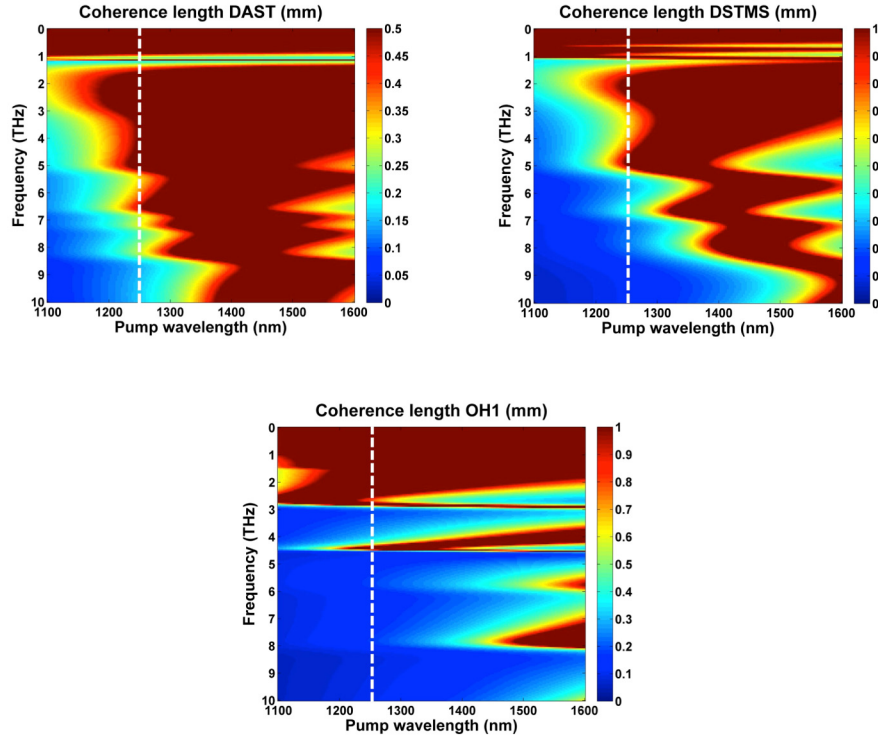


Fig. 1. Calculated coherence length for DAST, DSTMS and OH1 at different pump wavelengths and THz frequencies. As shown in all pictures the Cr:F emission wavelength (dashed white line) at 1250 nm gives rise to a coherence length comparable to the OPA typical wavelength range (1300-1600 nm).

As shown in Fig. 1, in the frequency range 1-10 THz, the velocity matching is optimal at pump around 1400-1500 nm in DAST and DSTMS. In OH1 the velocity matching is achieved mainly at low frequencies up to 3 THz with maximum coherence length for 1350 nm pump. As shown on the graph, reasonable coherence length is achieved at the Cr:F wavelength  $\lambda_{\text{Cr:F}} = 1250 \text{ nm}$  (Fig. 1, dashed lines). For DAST and DSTMS,  $l_c(\lambda_{\text{Cr:F}})$  is larger than 0.5 mm in the frequency range between 0.1 and 5 THz. At frequencies larger than 5 THz, for  $\lambda_{\text{Cr:F}}$  the phase matching is less favorable with respect to longer pump wavelengths. The calculations in Fig. 1 indicate that the Cr:F pump wavelength is even better suited for pumping OH1 with more than 1 mm coherence length in the frequency range 0.1-3 THz.

### 3. Results and discussion

Our experimental setup is described in [15]. In short, the Cr:forsterite system consists of a femtosecond oscillator followed by a multistage chirped pulse amplifier. Nd:YAG lasers operated at the fundamental wavelength (1064 nm) at repetition rate of 10 Hz are used to pump the amplifier stages and boost the Cr:F pulse energy up to 35 mJ after compression. The final pulses have 95 fs FWHM duration and 27 nm spectral bandwidth at around 1250

nm. The collimated beam is used to pump the various NOCs. After OR in NOC, the THz radiation is separated from the pump beam by means of several low pass filters. For the realization of a small focus, the THz beam is first expanded by an all-reflective telescope and successively focused by a short focal length parabolic mirror.

**Table 1. Nonlinear organic crystals – dimensions and THz performance using a Cr:F pump laser.**

Organic crystal	Thickness-Diameter (mm)	Maximum efficiency	Max. energy/fluence $\mu\text{J}/\text{cm}^2$	Emitted spectrum	Focus FWHM $\mu\text{m}$	Electric field
DAST	0.18-5	2.1%	62 $\mu\text{J}$ / 280 $\mu\text{J}/\text{cm}^2$	0.1-10 THz	490 $\mu\text{m}$	6.2 MV/cm
DSTMS	0.9-10	1.1%	150 $\mu\text{J}$ / 110 $\mu\text{J}/\text{cm}^2$	0.1-4 THz	210 $\mu\text{m}$	18 MV/cm
OH1	0.44-10	3.2%	270 $\mu\text{J}$ / 300 $\mu\text{J}/\text{cm}^2$	0.1-3 THz	440 $\mu\text{m}$	9.9MV/cm

For the present study single-piece NOCs of different size and type have been available. Information on the crystals (type, thickness and clear aperture) and the measured THz output characteristics, such as the maximum NIR-to-THz conversion efficiency and energy, the spectral characteristics, the minimum THz spot size (FWHM) and the peak electric field, are summarized in Table 1. The beam waist is measured with a microbolometer THz imager (NEC IR/V-T0831). After the focus the beam is re-collimated by a parabolic mirror and sent to a Michelson interferometer for spectral measurement. Energy, beam size and pulse duration allow to estimate the maximum electric field in the focus position [19].

When pumped by Cr:F the organic crystals provide NIR-to-THz conversion efficiency as large as of few percent. For the energy measurements, a pyroelectric sensor (SPI-D, Spectrum Detector Inc.) and a calibrated Golay cell (Tydex Inc.) have been used with an agreement between the detectors better than 10%.

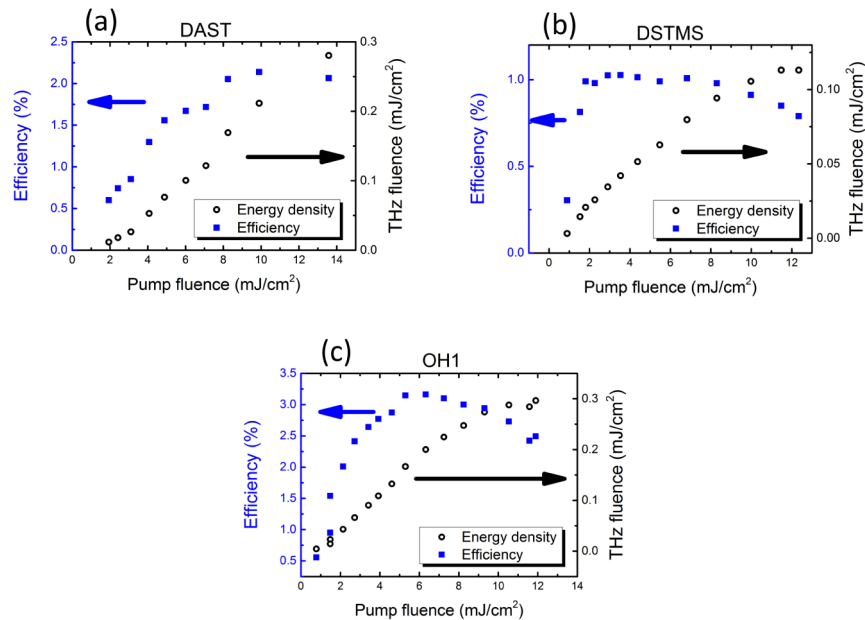


Fig. 2. Efficiency and emitted THz energy density from DAST, DSTMS and OH1 as function of the Cr:F fluence.

The emitted THz energy densities and the conversion efficiencies for the different NOCs are shown in Fig. 2. The dissimilar clear apertures of the NOCs, see Table 1, suggests a

comparison in terms of pump and THz fluence rather than absolute energy. In DAST, Fig. 2(a), the maximum conversion efficiency exceeds 2% at around  $10 \text{ mJ/cm}^2$  pump fluence. At higher laser energy density the onset of saturation and steady efficiency are observable. These results surpass previous efficiency reported for DAST with an OPA pumping scheme, as described for instance in [4]. The efficiency is higher with respect to the OPA pumping scheme. This is attributed to the more uniform beam profile in Cr:F, which permits optimal distribution of the pump energy [15]. Maximum energy density of  $0.28 \text{ mJ/cm}^2$  corresponds to THz pulse energy of  $62 \text{ }\mu\text{J}$ . In DSTMS, Fig. 2 (b), the efficiency curve saturates at a relatively low pump fluence of around  $2 \text{ mJ/cm}^2$  before it drops due to THz re-absorption and back conversion. These values are significantly lower than what has been reported from  $0.5 \text{ mm}$  thick partitioned DSTMS pumped by the same source [14]. The lower conversion efficiency can be ascribed to the larger thickness with stronger THz re-absorption and to the quality of the present crystal. In agreement with the coherence length calculations of Fig. 1, the Cr:F wavelength is well suited for optical rectification in OH1. This turns into record-high conversion efficiency, which exceeds 3.3% at pump fluence of  $5 \text{ mJ/cm}^2$ . The equivalent photon conversion efficiency of 480% indicates a cascading OR process of order close to 5 [1]. The maximum THz energy density exceeds  $0.3 \text{ mJ/cm}^2$  with potential to generate pulse energy larger than  $1 \text{ mJ}$  for large aperture crystals and high power laser.

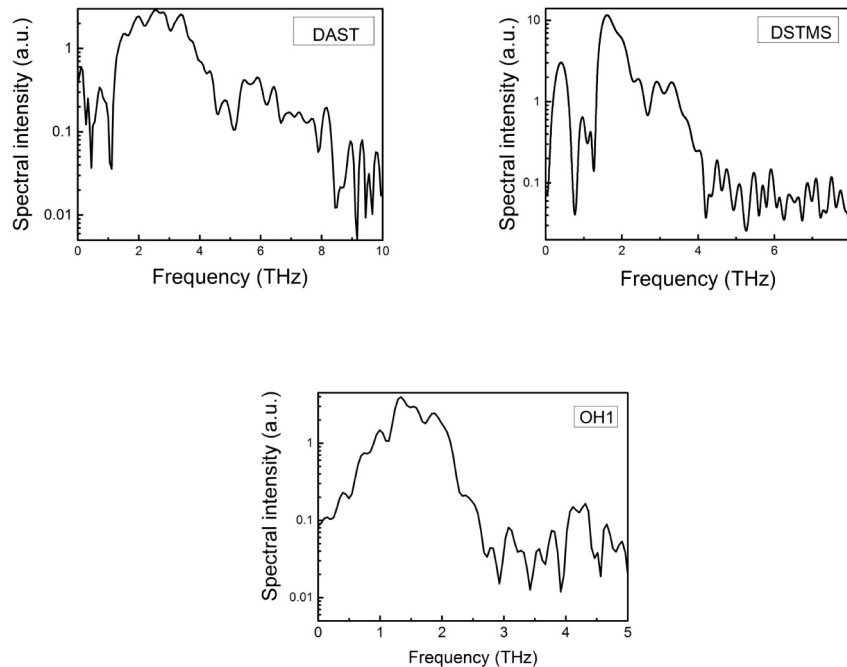


Fig. 3. Terahertz spectrum emitted by DAST, DSTMS and OH1 retrieved by first order autocorrelation in a THz Michelson interferometer.

The generated THz spectra are measured by means of a first order Michelson interferometer equipped with a THz-sensitive detector (Golay cell). Examples of spectra in DAST, DSTMS and OH1 when pumped at the maximum fluence of about  $12 \text{ mJ/cm}^2$  are shown in Fig. 3. The curves display the typical phonon active absorption characteristics of each organic compound [1–4]. The spectral measurements have been performed in ambient air inducing spectral modulation due to absorption in water vapor (relative humidity of 40%). The THz pulse produced in the thin DAST carries spectral components, which extends over several octaves [0.1-8 THz] while the emission from the DSTMS and OH1 gives rise to

narrower spectrum but still covering several octaves 0.1-4 THz and 0.1-3 THz respectively. The calculated spectra are in good agreement with the coherence length presented in Fig. 1. The multi-octave spectral contents are comparable with the one achieved in NOCs with OPA pumping [1-4].

Pumped by a collimated beam, NOCs emit THz radiation in forward direction with symmetric spatial intensity profile and minor wavefront aberration. This allows for tight focusing. In the experimental setup a 1:2 telescope expands the THz beam before the final parabolic mirror (f-number = 2.5,  $f = 5$  cm). The profile in the focus is symmetric and well approximated by a two dimensional Gaussian distribution. Figure 4 shows the beam waist and the corresponding cross-sections for DSTMS. The spot is circular with a size at half maximum of 212  $\mu\text{m}$ . Similar focus shape but somehow bigger size are achieved in OH1 and DAST crystals, Table 1. The THz beam waist for the OH1 is larger due to the predominance of low frequencies mainly located below 3 THz. In the case of DAST the THz focus size is larger due to the smaller crystal clear aperture and larger numerical aperture of the focusing system (f-number = 5).

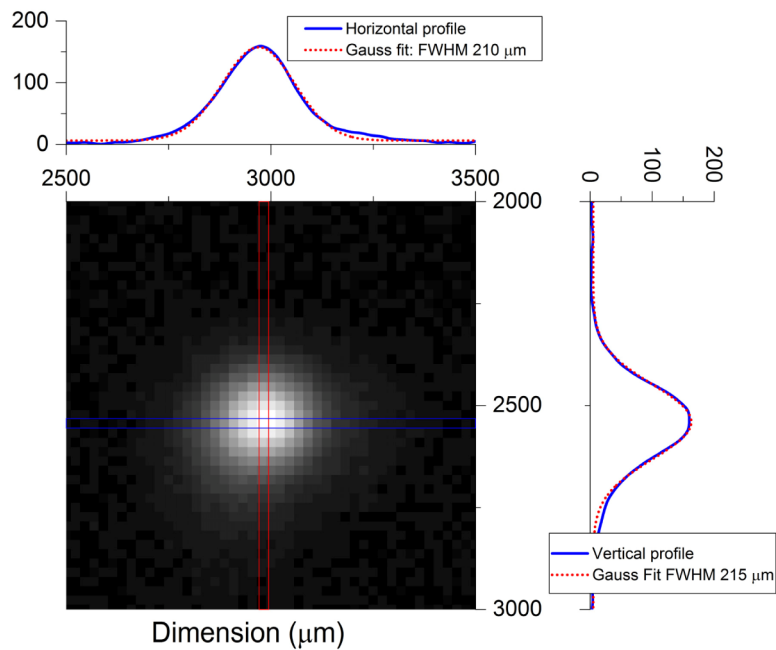


Fig. 4. THz beam profile in the beam waist for DSTMS.

The THz field strengths reported in Table 1 are determined from the measured THz pulse energy, the THz beam size at the focus and the pulse duration [19]. In our simple setup, state of the art field strength is reached without extensive optimization. As mentioned before, higher frequencies for DAST and DSTMS are focused more tightly, resulting in higher electric (magnetic) fields of 6 and 18 MV/cm (2 and 6 Tesla), respectively. Despite the highest pulse energy achieved in OH1, the dominantly lower THz frequency components limit the achievable minimum spot size to about half a millimeter FWHM and consequently the electric and magnetic peak field to about 10 MV/cm and 3 Tesla, respectively.

In principle, the field can be substantially higher for an optimized focusing system. As recently shown, the NOC-based THz sources provide radiation that can be focused to a diffraction-limited, lambda-cubic spot size using small f-number focusing optics and wavefront optimization [20]. This opens new opportunities in nonlinear terahertz experiments.

### 3. Conclusion

We investigated high-field THz generation in organic crystals DSTMS, DAST and OH1 by optically rectifying a femtosecond Cr:fosterite laser pulse at 10 Hz repetition rate. We report on coherence length, emitted THz energy and spectrum as well as conversion efficiency and beam profile. Our results suggest that the Cr:F laser technology is well suited for optical rectification in the most common organic crystals with emission between 0.1 and 6 THz, due to the smooth and Gaussian-like pump profile and the relatively long coherence length. In OH1 we demonstrate maximum conversion efficiency as high as 3.2% that corresponds to energy per pulse up to 270  $\mu$ J. The record-high conversion value corresponds to photon conversion efficiency of 480%, due to higher-order cascaded optical rectification. In all the investigated crystals the THz beam could be focused to a few hundred  $\mu$ m spot size resulting in maximum peak electric and magnetic field up to 18 MV/cm and 6 Tesla respectively.

### Acknowledgments

This research has been supported by the Swiss National Science Foundation (SNSF) under grant no. 200021\_146769 and SwissFEL and was performed at the Joint Institute of High Temperatures of the Russian Academy of Sciences. C.P.H. acknowledges association to the National Center of Competence in Research-Molecular Ultrafast Science and Technology (NCCR-MUST) and acknowledges financial support from SNSF under grant no. PP00P2\_150732.